



A recoverable sandwich phosphorotungstate stabilized palladium (0) catalyst for aerobic oxidation of alcohols in water



Lijuan Chen^{a,b,*}, Tao Feng^c, Pengfei Wang^c, Ziwen Chen^a, Riqing Yan^a, Bo Liao^{a,b},
Yujun Xiang^a

^a School of Chemistry and Chemical Engineering, Hunan University of Science and Technology, Xiangtan, PR China

^b Key Laboratory of Theoretical Chemistry and Molecular Simulation of Ministry of Education, Hunan University of Science and Technology, Xiangtan, PR China

^c School of Energy Source, Hunan University of Science and Technology, Xiangtan, PR China

ARTICLE INFO

Article history:

Received 24 March 2016

Received in revised form 18 May 2016

Accepted 10 June 2016

Available online 13 June 2016

Keywords:

Mesoporous aluminophosphate

Polyoxometalates

Alcohol oxidation

Palladium nanoparticle

ABSTRACT

The preparation, characterization and catalytic properties of tetra metal substituted sandwich phosphorotungstate $[M_4(H_2O)_2(PW_9O_{34})_2]^{10-}(M_4P_2W_{18}, M^{2+} = Fe^{2+}, Co^{2+}, Mn^{2+}, Cu^{2+}, VO^{2+})$ stabilized Pd nanoparticles, which were in-situ encapsulated in mesoporous aluminum phosphate (mAPO) by a one-pot method, were demonstrated for aerobic oxidation of alcohol in water. The synthesized catalysts were characterized with N₂ adsorption, XRD, TEM, FT-IR and UV-vis. TEM analysis revealed that Pd-M₄P₂W₁₈/mAPO thus obtained has a mean palladium particle size of less than 5 nm. The solid Pd-M₄P₂W₁₈/mAPO catalysts exhibit excellent activity for aerobic oxidation of benzyl alcohols in water without any base additives. It was found the introduced M₄P₂W₁₈ polyoxanions encapsulated palladium nanoparticles as both stabilizing agent and promoters, leading to enhanced activity and recyclability of palladium catalyst. The recycling test of representative Pd-(VO)₄P₂W₁₈/mAPO for oxidation of benzyl alcohol suggested no significant decrease in activity and selectivity even after twelve times of successive reactions. This novel heterogeneous catalyst composed of polyoxometalates stabilized palladium nanocatalysts and mesoporous aluminophosphate can also be extended to the selective oxidation of various alcohols.

© 2016 Elsevier B.V. All rights reserved.

1. Introduction

The oxidation of alcohols is one of the most fundamental transformations of great commercial and research significance because the corresponding aldehyde/ketone products serve as important intermediates in the fine chemicals and pharmaceutical industries. The stoichiometric oxidants like KMnO₄ or CrO₃ are conventionally used to accomplish this transformation [1]. However, these processes usually produce large amount of toxic inorganic salts waste and the yields of the desired product aldehyde/ketone are often low. With the ever-increasing environmental concerns, the development of heterogeneous transition-metal based catalysts for aerobic oxidation of alcohols using air or oxygen as oxidant has

attracted much attention [2,3]. Water is an ideal solvent for this protocol because it can avoid explosions and the hazards associated with the use of oxidisable organic solvents under oxygen pressure. Among these studies, palladium-based homogeneous or heterogeneous catalysts show promising activity in aqueous solution under mild conditions, a number of palladium-based catalysts in the form of metal complexes or nanoparticles have been investigated for this purpose [4–11]. Although the progress for palladium catalyzed aerobic oxidation of alcohols is notable, palladium catalysts often suffer from easy agglomeration and formation of palladium black that cause their deactivation in many cases. Moreover, in many aerobic alcohol oxidation systems using noble metal based catalysts, base additives are often necessitated to improve conversion of alcohol and selectivity for corresponding carbonyl product. According to literature, the base additives can facilitate the dehydrogenation of alcohol and promote the β-H elimination of a dissociated alcohol on the Pd surface [9]. However, the alkaline environment under oxygen atmosphere is harmful to the stability

* Corresponding author at: School of Chemistry and Chemical Engineering, Hunan University of Science and Technology, Xiangtan, PR China.

E-mail address: ljchen11@163.com (L. Chen).

of palladium catalyst, leading to an easier deactivation of palladium catalyst due to over-oxidation and poisoning [6]. In this context, the development of palladium-based heterogeneous catalysts with improved recyclability for base-free aerobic oxidation of alcohols in water is desirable in recent years.

For supported Pd nanoparticles catalyst, the morphology and particle size control of Pd nanoparticles is an important factor affecting the recyclability of catalysts. The previous studies indicate that the catalytic activity of nano-sized metallic Pd for aerobic oxidation of alcohols is dependent on the size and morphology of the surface Pd nanoparticles, and the Pd nanoparticles with particle size of a few nanometers show the highest activity [12,13]. However, it is well known that the nanoparticles of small particle size are very mobile and thermodynamically prone to agglomerate into larger inactive particles [14]. Thus the improved recyclability of heterogeneous palladium catalysts is dependent on the better control and maintenance of the particle size of Pd nanoparticles in desired range during the catalyst preparation and the sequent catalytic reactions. The strategies preventing the growth of Pd nanoparticles that are widely used in heterogeneous palladium catalysts includes combinations with the promoter metal such as Bi, Pb or Au, surface functionalization of support in order to strengthen the bonding of Pd nanoparticles and confinement of Pd nanoparticles in nano-sized channels of supports [15–22]. However, these methods often suffer from some disadvantages, for example, some promoters such as Bi and Pb are not green agents, Pd and Au needed to form a desired alloy phase to generate the enhanced activity, the procedures for surface functionalization of support and post-treatment are complicated and part of active species that located in small mesopores is difficultly contactable by substrate molecules.

Recently, one of the important applications of polyoxometalates emerged in metal clusters stabilization [23]. D'souza and coworkers reported a simple synthesis of Krebs type polyoxoanions $[(\text{TBA})_4\text{H}_4\text{M}_4(\text{H}_2\text{O})_{10}(\text{XW}_9\text{O}_{33})_2]$ stabilized Pd, Au and Ag metal colloidal systems, the metal particle size in these systems were well controlled in a narrow range and remained unchanged for approximately three/six months in solution media [24]. On the other hand, polyoxometalates are a kind of efficient catalyst for selective oxidation of organic chemicals, in palladium catalyzed oxidation reactions, the combinations with polyoxometalates can effectively promote to the activity of palladium catalysts [24–31]. Neumann and co-workers reported a Pd^{II} -polyoxometalate catalyst by attaching a sandwich type $[\text{WZn}_3(\text{H}_2\text{O})_2][(\text{ZnW}_9\text{O}_{34})_2]$ polyoxoanion to a Pd^{II} center for aerobic oxidation of primary aliphatic alcohols, this group also reported a polyoxometalate appended with alkylthiol tethers $[\text{SiW}_{11}\text{O}_{40}(\text{SiCH}_2\text{CH}_2\text{CH}_2\text{SH})_2]$ stabilized Pd nanoparticles catalysts for liquid aerobic oxydehydrogenation of vinylcyclohexene and vinylcyclohexane to styrene [29,30]. Zhang and coworkers reported the enhanced electrocatalytic properties of Pd and Pt nanoparticles/polyoxometalates/graphene tri-component nanohybrids for methanol and formic acid oxidation [31]. In these systems, the synergic catalysis of Pd species and polyoxometalates lead to improved conversion and selectivity, the promotion effect of polyoxometalates is most likely related to their electron-accepter properties and oxygen-activating capability [32].

Inspired by the above studies, here we reported a integrated catalytic system based on sandwich type polyoxometalates $[\text{M}_4(\text{H}_2\text{O})_2(\text{PW}_9\text{O}_{34})_2]^{10-}$ ($\text{M}^{2+} = \text{Fe}^{2+}, \text{Co}^{2+}, \text{Mn}^{2+}, \text{Cu}^{2+}, \text{VO}^{2+}$) and palladium nanoparticles through in situ encapsulation of pre-synthesized $\text{M}_4\text{P}_2\text{W}_{18}$ stabilized palladium nanoparticles in mesoporous aluminophosphate by a sol-gel method. The synthesized catalyst showed high catalytic performance for aerobic oxidation of alcohols in water. The catalyst also showed enhanced stability and recyclability compared with other heterogeneous palladium catalysts without modification of polyoxometalates.

2. Experimental

2.1. Chemicals and methods

Powder X-ray diffractions of samples were recorded on a Brucker AXS D8 Advance diffractometer using $\text{Cu K}\alpha$ radiation. TEM images were recorded on a JEM 3010 TEM operated at 200 kV. More than 100 particles for each sample were randomly counted to determine the particle size distributions. N_2 adsorption and desorption isotherms were obtained on a micromeritics ASAP 2010 instrument at 77 K, samples were degassed at 120 °C for 5 h under high vacuum prior to measurements. Surface areas and pore distribution were calculated by BET and BJH methods, respectively. Elemental analysis of samples was performed with an inductively coupled plasma-optical emission spectrophotometer Shimadzu ICPs-7500 to determine the amount of Pd and polyoxometalates in heterogeneous catalyst. IR spectra were recorded on KBr pellets by a Nicolet Niclet 6700 spectrophotometer. UV-vis spectra of samples were obtained with Perkin-Elmer Lambda-35 spectrophotometer.

K_2PdCl_4 was used as Pd precursor. Sodium tungstate dihydrate, phosphoric acid (85%), cobalt nitrite hexahydrate, manganese acetate tetrahydrate, vanadium sulfate heptahydrate and ferrous sulfate pentahydrate were used as the sources of W, P, Co, Mn, V and Fe for the synthesis of the tetra metal substituted tungstophosphates. To prepare mesoporous aluminophosphate, aluminium isopropoxide and phosphoric acid were used as the sources of aluminum and phosphorous, respectively, and hexadecylamine (HDA) was used as template. All the chemicals were analytical grade and used as received without further treatment.

2.2. Preparation of sandwich tungstophosphates

The potassium salts of sandwich polyoxoanions $[\text{M}_4(\text{H}_2\text{O})_2(\text{PW}_9\text{O}_{34})_2]^{10-}$ ($\text{M}^{2+} = \text{Co}^{2+}, \text{Fe}^{2+}, \text{Mn}^{2+}, \text{VO}^{2+}$) were synthesized by the reaction of $\text{Na}_9\text{PW}_9\text{O}_{34}$ with the corresponding soluble metal salts in water and precipitation with solid potassium chloride, as described by the published literature [33]. The purity of the samples was tested by IR and NMR spectroscopy.

2.3. In-situ encapsulation of $\text{M}_4\text{P}_2\text{W}_{18}$ stabilized Pd nanoparticles in mesoporous aluminophosphate

The pre-synthesized $\text{M}_4\text{P}_2\text{W}_{18}$ stabilized Pd nanoparticles was incorporated in mesoporous aluminophosphate by a hydrothermal method from a gel composition of 0.0057 K_2PdCl_4 : 0.0011 $\text{M}_4\text{P}_2\text{W}_{18}$: Al_2O_3 : P_2O_5 : 1.2HDA: 65ethanol: 300 H_2O . In a typical synthesis, $\text{M}_4\text{P}_2\text{W}_{18}$ stabilized Pd nanoparticles colloidal solution were obtained by the following procedures: the mixture of 2.5 mL of $\text{M}_4\text{P}_2\text{W}_{18}$ (10 mM) and 12.6 mL of K_2PdCl_4 (10 mM) aqueous solution was stirred for 5 min, then Pd^{II} was reduced to Pd^0 with 3 mL of freshly prepared 0.1 M NaBH_4 by ultrasonication for 10 min. The $\text{M}_4\text{P}_2\text{W}_{18}$ stabilized Pd nanoparticles colloidal solution was then added to the precursor solution composed of 2.24 g of aluminium isopropoxide, 1.06 g of orthophosphoric acid and 1.32 g of hexadecylamine in 11.5 g of water and 27.8 g of ethanol. The resulting gel of the above composition was stirred for 3 h at room temperature and then transferred into a Teflon lined autoclave in an oven at 120 °C for 24 h. After cooling, the solid in gray color was filtered, washed thoroughly with distilled water and dried in air. The template was removed by a combined solvent extraction and calcination method. For extraction procedures, 1 g of the above dried solid was stirred in 40 mL of 0.05 M HCl/ethanol at room temperature for 15 min and washed with ethanol, the process repeated for five times. The solid product after extraction was dried at 80 °C overnight, and then calcinated at 400 °C for

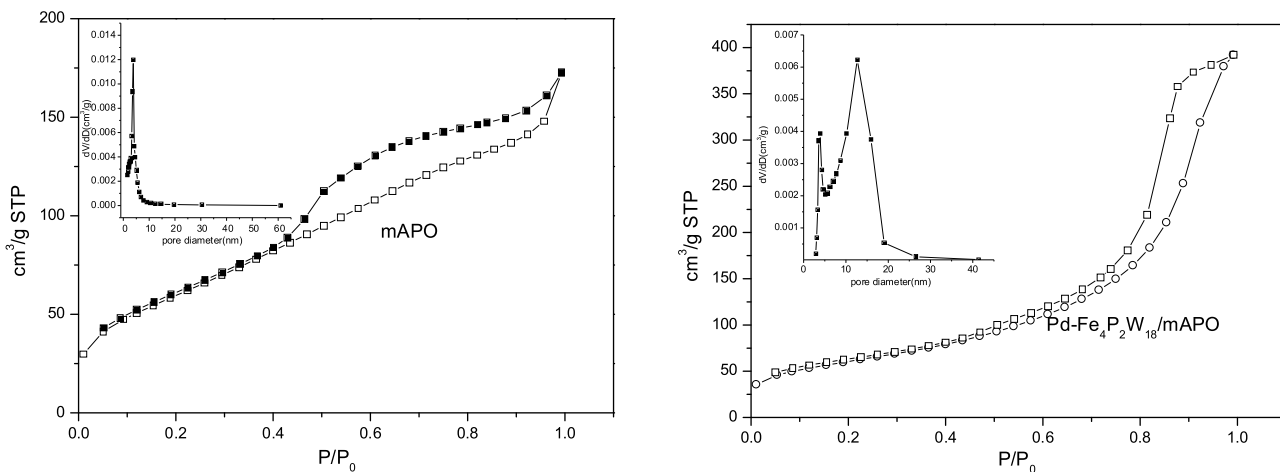


Fig. 1. N₂ absorption-desorption isotherms and insert pore size distribution of (a) mAPO and (b) Pd-Fe₄P₂W₁₈/mAPO.

5 h with a temperature ramp rate of 1 °C/min. The ICP results of sample after calcination indicates that the Pd amount is near to 1 wt% (0.97%) based on aluminophosphate and the molar ratio of palladium to M₄P₂W₁₈ is near to 5:1. The catalysts prepared by this process are denoted as Pd-M₄P₂W₁₈/mAPO.

In order to make comparative studies, two heterogeneous palladium catalyst, Pd/mAPO (1 wt%) and M₄P₂W₁₈ + Pd/mAPO were prepared. Pd/mAPO was prepared through adsorption of K₂PdCl₄ solution on mesoporous aluminophosphate and reduction. M₄P₂W₁₈ + Pd/mAPO was prepared through adsorption of M₄P₂W₁₈ solution on Pd/mAPO (1 wt%). The polyoxometalates and palladium content in these two heterogeneous catalysts were adjusted to be same as that in Pd-M₄P₂W₁₈/mAPO.

2.4. Catalytic application

The reactions were performed in a two-neck round bottom flask, provided with a reflux condenser and an electrically controlled magnetic stirrer. In typical conditions, 30 mg of solid catalyst, 1 mmol of alcohol in 10 mL of distilled water was mixed in the flask, and oxygen gas was introduced into the flask from an O₂ balloon under atmospheric pressure. The reaction was started by placing the flask into an oil bath preheated to the reaction temperature and starting magnetic stirring. After the given reaction time, the catalyst was separated from the solution by filtration, the reaction solution was extracted with diethyl ether twice, 5 mL for each time, and the combined organic layer was dried with MgSO₄, analyzed by GC to determine the conversion and selectivity.

3. Results and discussion

3.1. Structural features of catalysts

The N₂ adsorption-desorption isotherms and the corresponding pore diameter distribution of mesoporous aluminophosphate (mAPO) and the representative Fe₄P₂W₁₈-Pd⁰/MAPO supported catalyst were presented in Fig. 1. Both are IV type isotherms with a pronounced H₃ hysteresis loop evidenced of its mesoporous structure. A sharp step increase in the relative pressure range of 0.5–0.8 was observed in the isotherm of mAPO due to the capillary condensation of N₂ inside the mesopores. The increase step shifted to higher P/P₀ for Pd-Fe₄P₂W₁₈/mAPO, suggesting formation of larger pore sizes in Fe₄P₂W₁₈-Pd/mAPO composite material. The Barrett-Joyner-Halenda (BJH) plot of Fe₄P₂W₁₈-Pd/MAPO reveals a wider pore distribution with two types of mesopores, the smaller mesopores centered at 3.8 nm and larger mesopores centered at

Table 1
Properties of mesoporous aluminophosphate and various M₄P₂W₁₈-Pd/MAPO samples.

| sample | S _{BET} (m ² /g) | Pore volume (V _P /cm ³ g ⁻¹) | pore diameter (D _P /nm) |
|---|--------------------------------------|--|------------------------------------|
| mAPO | 204 | 0.43 | 3.8 |
| Pd-Fe ₄ P ₂ W ₁₈ /mAPO | 216 | 0.50 | 3.8+12.6 |
| Pd-Mn ₄ P ₂ W ₁₈ /mAPO | 210 | 0.45 | 3.9+12.4 |
| Pd-Co ₄ P ₂ W ₁₈ /mAPO | 214 | 0.48 | 3.9+12.7 |
| Pd-Cu ₄ P ₂ W ₁₈ /mAPO | 216 | 0.50 | 4.0+12.8 |
| Pd-(VO) ₄ P ₂ W ₁₈ /mAPO | 218 | 0.52 | 4.0+12.6 |

12.6 nm. The chain alkyl amine surfactant and polyoxometalates stabilized Pd⁰ clusters can be combined through formation of electrostatic bonding NH₃⁺...polyoxoanion, the subsequent condensation with the sol-gel precursor aluminium isopropoxide and orthophosphoric acid leads to a more disordered mesostructure with wide pore distribution. After the condensation, the M₄P₂W₁₈ stabilized Pd⁰ clusters are uniformly dispersed in the framework of mesoporous aluminophosphate. The present of large mesopores in Pd-Fe₄P₂W₁₈/mAPO is advantageous to the substrate molecule entering into the pores and contacting with active centers inside the mesopores. The Brunauer-Emmett-Teller specific area (S_{BET}), total pore volume and mesopore diameter of other Pd-M₄P₂W₁₈/mAPO and mAPO are summarized in Table 1.

Fig. 2 is the UV-vis spectra of samples. Fe₄P₂W₁₈ was selected as an example to reflect the chemical transformation during the preparation of Pd-M₄P₂W₁₈/mAPO. The plots a–c are UV-vis spectra of Fe₄P₂W₁₈, K₂PdCl₄ and Fe₄P₂W₁₈ protected Pd colloid (Fe₄P₂W₁₈-Pd⁰) in diluted aqueous solution, respectively. A strong adsorption band at 206 nm is observed in the UV-vis spectra of K₂PdCl₄, which was attributed to ligand-to-metal charge transition of Pd²⁺ ion in tetrahedral coordination [34]. This adsorption band disappears in UV-vis spectra of Fe₄P₂W₁₈-Pd⁰, indicating the complete reduction of Pd²⁺ to Pd⁰. An absorption band at about 250 nm in the UV-vis spectra of Fe₄P₂W₁₈ and Fe₂P₂W₁₈-Pd⁰ is attributed to the charge transfer associated with heteropolytungstate anion PW₉O₃₄⁹⁻. A weak absorbance in the range of 300–400 nm, shoulder at 350 nm in the UV-vis spectra of Fe₄P₂W₁₈ is probably assigned to the d-d transition of iron (II) ions. The plots d and e in Fig. 2 represent the UV-vis spectra of pure mAPO and Pd-Fe₄P₂W₁₈/mAPO, respectively. Both show similar and very strong absorption bands in the 200–350 nm wavelength region, which was attributed to the Al in tetrahedral coordination with Al—O—P bonds, [Al(OP)₄]. A small hump after 350 nm can be observed in the UV-vis spectra of Pd-Fe₄P₂W₁₈/mAPO, which may arise due to the pres-

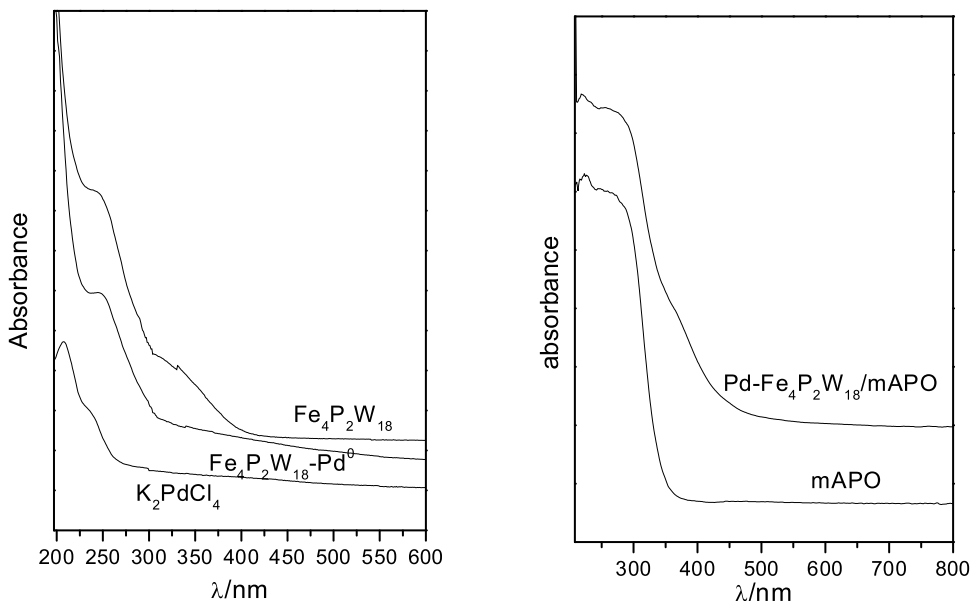


Fig. 2. UV-vis spectra of aqueous solution of (a) K₂PdCl₄, (b) Fe₄P₂W₁₈-Pd⁰, (c) Fe₄P₂W₁₈ and solid samples: (d) mesoporous aluminophosphate (mAPO) and Pd-Fe₄P₂W₁₈/mAPO(e).

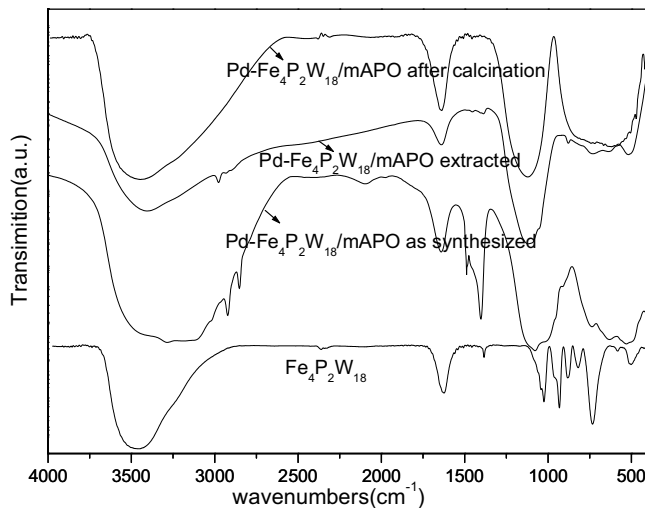


Fig. 3. IR spectra of samples(a) Fe₄P₂W₁₈; (b) Pd-Fe₄P₂W₁₈/mAPO-CTAB; (c) Pd-Fe₄P₂W₁₈/mAPO-CTAB(extracted); (d) calcinated Pd-Fe₄P₂W₁₈/mAPO.

ence of heteropolyanion, its absorbance shifts to higher wavelength compared to free Fe₄P₂W₁₈ in water solution, the shift is related to the interaction of Fe₄P₂W₁₈ with aluminophosphate.

The success in incorporating M₄P₂W₁₈ stabilized Pd nanoparticles in mAPO was confirmed with FT-IR spectroscopy. The FT-IR spectra of Fe₄P₂W₁₈ and Pd-Fe₄P₂W₁₈/mAPO samples (as-prepared, HCl/ethanol extracted and calcined) are shown in Fig. 3. The bands at 3500 and 1640 cm⁻¹ are attributed to the asymmetric OH stretching vibration and bending vibration of water, respectively. The bands in wavenumber range of 1250–700 cm⁻¹ in FT-IR spectra of Fe₄P₂W₁₈ are attributed to the vibration frequencies of P=O(1020 cm⁻¹), W=O(926 cm⁻¹), W—O—W and W—O—Fe bands (876, 813 and 725 cm⁻¹), respectively, in agree with previously published values [35]. However, in the FT-IR spectra of Pd-Fe₄P₂W₁₈/mAPO samples, these bands are not clearly visible due to overlapping with the bands of mAPO in the wavenumber range of 1100–400 cm⁻¹. In the FT-IR of as-prepared Pd-Fe₄P₂W₁₈/mAPO, bands at 1512 cm⁻¹ and 2800–3000 cm⁻¹ are assigned to the C—H

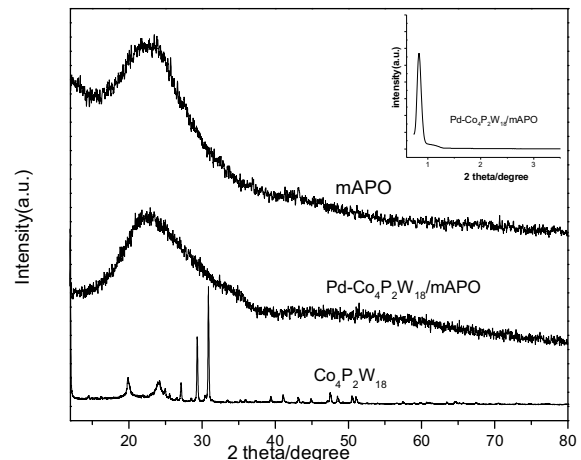


Fig. 4. XRD patterns of the samples in wide-angle region. (a) Co₄P₂W₁₈ (b) Pd-Co₄P₂W₁₈/MAPO (c) mAPO. (the insert is the low-angle XRD of (b)).

stretching of surfactant, which undergo a sharp decrease in intensity in the FT-IR of HCl/ethanol extracted Pd-Fe₄P₂W₁₈/mAPO and disappear in the FT-IR of Pd-Fe₄P₂W₁₈/mAPO after calcinations. The FT-IR spectra of other Pd-M₄P₂W₁₈/mAPO samples synthesized with different polyoxometalates shows similar patterns to that of Pd-Fe₄P₂W₁₈/mAPO.

The XRD patterns of Co₄P₂W₁₈, mAPO and Pd-Co₄P₂W₁₈/mAPO are shown in Fig. 4. The wide angle powder XRD patterns of mAPO and Pd-Co₄P₂W₁₈/mAPO exhibit a broad peak in 2θ ranges of 10–30°, indicating their amorphous nature. In Pd-Co₄P₂W₁₈/mAPO, no individual crystalline peaks of Co₄P₂W₁₈ and metallic Pd are observed, indicating Co₄P₂W₁₈ and Pd nanoparticles remain high dispersion on mAPO. The small angle XRD of Pd-Co₄P₂W₁₈/mAPO (Fig. 4, insert) exhibit an intense reflection at 0.82° and a very weak reflection at 1.17°, corresponding to a d-spacing of 10.7 nm. These low angle diffraction peaks signify the formation of mesopores, the single intense peak in low angle range suggests the pores are arranged with large irregularity in these materials.

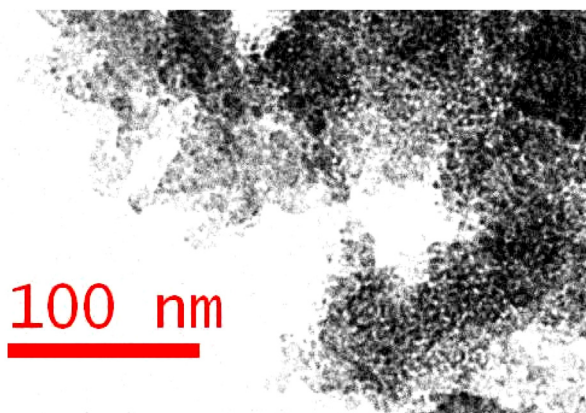


Fig. 5. TEM image of mesoporous Pd-(VO)₄P₂W₁₈/mAPO using hexadecylamine as templating agent after extraction and then calcined at 400 °C for 5 h (scale bar = 100 nm).

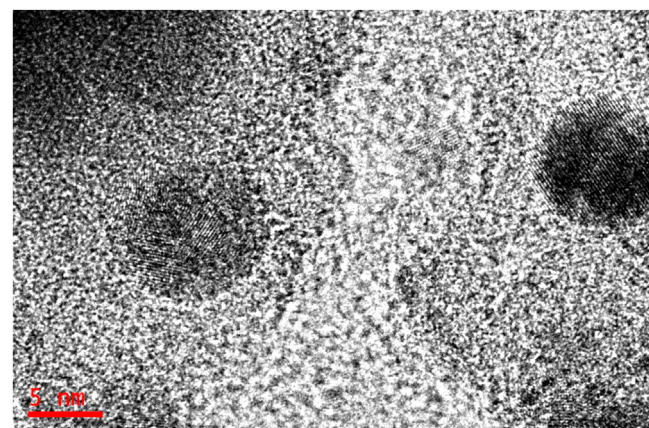


Fig. 7. High-resolution TEM image of Pd-(VO)₄P₂W₁₈/mAPO showing the crystal structure of Pd nanoparticles (scale bar = 5 nm).

TEM images of representative Pd-(VO)₄P₂W₁₈/mAPO of different magnification are shown in Figs. 5–7. As seen in Fig. 5, the mesopores of Pd-(VO)₄P₂W₁₈/mAPO, seen as low electron density spots in specimen, are distributed randomly to form a wormhole-like disordered mesostructure. As seen in Fig. 6, the freshly prepared Pd-(VO)₄P₂W₁₈/mAPO exhibits Pd particle size distribution from 1.8 to 4.5 nm with the mean Pd particle size

3.0 nm, the Pd-(VO)₄P₂W₁₈/mAPO used for four times exhibits Pd particle size distribution from 2.3 to 5.4 nm with mean Pd particle size 3.7 nm. The comparison between the fresh and recovered Pd-(VO)₄P₂W₁₈/mAPO indicates not obvious variation in particle size and dispersion state before and after reaction. The high-resolution TEM image of Pd-(VO)₄P₂W₁₈/mAPO in Fig. 7 confirms the crys-

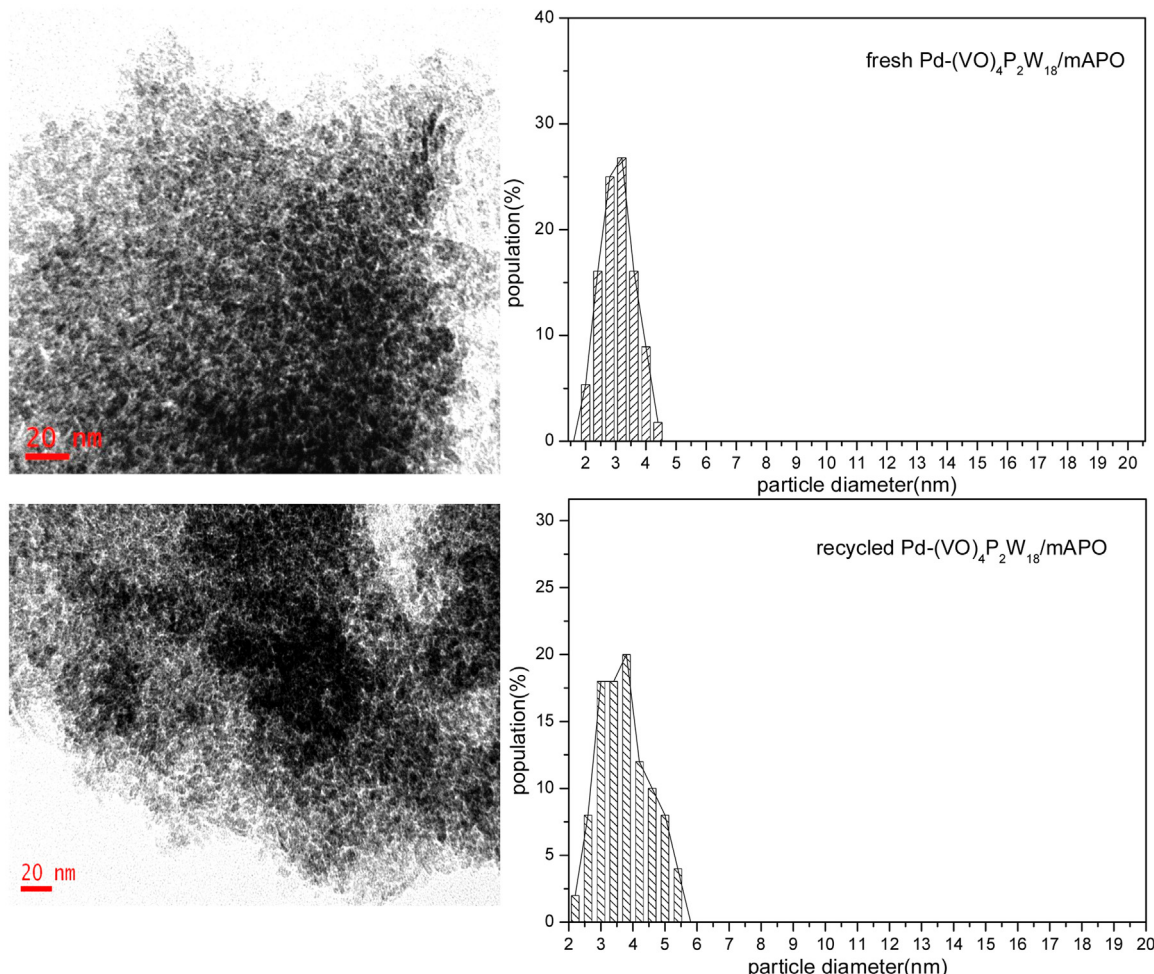


Fig. 6. Typical TEM images and Pd nanoparticle size distribution of (A) freshly prepared Pd-(VO)₄P₂W₁₈/mAPO and (B) Pd-(VO)₄P₂W₁₈/mAPO used for four successive runs in the oxidation of benzyl alcohol (scale bar = 20 nm).

Table 2
aerobic oxidation of benzyl alcohol using various catalysts.^a

| Entry | Catalysts | mol% Pd | mol% M ₄ P ₂ W ₁₈ | Conv. (%) ^b | Select. (%) |
|-------|--|---------|--|------------------------|-----------------|
| 1 | none | — | — | — | — |
| 2 | mAPO | — | — | 4.8 | 99 |
| 3 | Pd/mAPO | 0.2 | — | 51.6 | 96 ^c |
| 4 | Fe ₄ P ₂ W ₁₈ /mAPO | — | 0.04 | 10.5 | 98 |
| 5 | Mn ₄ P ₂ W ₁₈ /mAPO | — | 0.04 | 8.0 | 98 |
| 6 | Cu ₄ P ₂ W ₁₈ /mAPO | — | 0.04 | 9.2 | 98 |
| 7 | Co ₄ P ₂ W ₁₈ /mAPO | — | 0.04 | 10.7 | 98 |
| 8 | (VO) ₄ P ₂ W ₁₈ /mAPO | — | 0.04 | 11.2 | 98 |
| 9 | Pd-Fe ₄ P ₂ W ₁₈ /mAPO | 0.2 | 0.04 | 66.9 | 99 |
| 10 | Pd-Mn ₄ P ₂ W ₁₈ /mAPO | 0.2 | 0.04 | 63.3 | 99 |
| 11 | Pd-Cu ₄ P ₂ W ₁₈ /mAPO | 0.2 | 0.04 | 65.3 | 99 |
| 12 | Pd-Co ₄ P ₂ W ₁₈ /mAPO | 0.2 | 0.04 | 67.3 | 99 |
| 13 | Pd-(VO) ₄ P ₂ W ₁₈ /mAPO | 0.2 | 0.04 | 68.6 | 99 |
| 14 | Fe ₄ P ₂ W ₁₈ + Pd/mAPO | 0.2 | 0.04 | 62.2 | 99 |
| 15 | Mn ₄ P ₂ W ₁₈ + Pd/mAPO | 0.2 | 0.04 | 60.4 | 99 |
| 16 | Cu ₄ P ₂ W ₁₈ + Pd/mAPO | 0.2 | 0.04 | 61.1 | 99 |
| 17 | Co ₄ P ₂ W ₁₈ + Pd/mAPO | 0.2 | 0.04 | 62.4 | 99 |
| 18 | (VO) ₄ P ₂ W ₁₈ + Pd/mAPO | 0.2 | 0.04 | 63.2 | 99 |

^a Reaction conditions: 1 mmol benzyl alcohol in 10 mL water, 1 atm of O₂, 30 mg of catalyst, 80 °C, 600 rpm, 3 h.

^b Determined by GC.

^c Toluene was detected as byproduct.

talline nature of Pd nanoparticles, it also reveals that the particles are spherical in shape.

3.2. Catalytic activity results

3.2.1. Aerobic oxidation of benzyl alcohol in water

The catalytic activities of different heterogeneous catalysts such as mAPO, Pd/mAPO, Pd-M₄P₂W₁₈/mAPO and M₄P₂W₁₈ + Pd/mAPO were evaluated for aerobic oxidation of benzyl alcohol in water, and the results are summarized in Table 2. As shown in Table 2, the reaction can't proceed in the absence of catalyst, and mAPO affords 4.8% of conversion (Table 2, entries 1 and 2). The activity of mAPO for aerobic oxidation of benzyl alcohol was probably associated with its solid bifunctional acid-base properties [36]. With 0.2 mol% Pd to benzyl alcohol, Pd/mAPO (1 wt%) afforded a benzyl alcohol conversion of 51.6% within 3 h (Table 2, entry 3). Compared with Pd/mAPO, the palladium catalysts combined with polyoxometalates exhibited enhanced activity, the enhanced activity is related to the contribution of polyoxometalates component in catalytic system, the previous studies have demonstrated that the multinuclear sandwich complexes based on trivacant Keggin anion [PW₉O₃₄]⁹⁻ is active to O₂ or H₂O₂-based oxidations [37,38]. Under the reaction conditions described in Table 2, the contribution of polyoxometalates component in catalyst to the conversion of benzyl alcohol is around 10% (Table 2, entries 4–8).

Under the same reaction conditions, Pd-M₄P₂W₁₈/mAPO is more active than M₄P₂W₁₈ + Pd/mAPO. The higher catalytic activity of Pd-M₄P₂W₁₈/mAPO is related to its more efficient synergic catalysis of M₄P₂W₁₈ and Pd nanoparticles. The pre-synthesis of M₄P₂W₁₈ stabilized Pd nanoparticles and in-situ incorporation of M₄P₂W₁₈ stabilized Pd nanoparticles in the mesoporous aluminophosphate by hydrothermal method lead to a closer contact of M₄P₂W₁₈ and Pd nanoparticles in Pd-M₄P₂W₁₈/mAPO, the synergic catalysis derived from the interaction of polyoxometalates and palladium metal can produce an enhanced activity and selectivity [5]. Furthermore, under the stabilization of polyoxometalates and protection of mesoporous aluminophosphate, Pd nanoparticles with small size in Pd-M₄P₂W₁₈/mAPO remain high dispersion on mesoporous aluminophosphate, showing a better activity for aerobic oxidation of alcohols. As presented in Fig. 8, the substituted metal in M₄P₂W₁₈ affected the activity of M₄P₂W₁₈-Pd⁰/mAPO, VO²⁺ substituted M₄P₂W₁₈ showed relatively higher activity than other metal

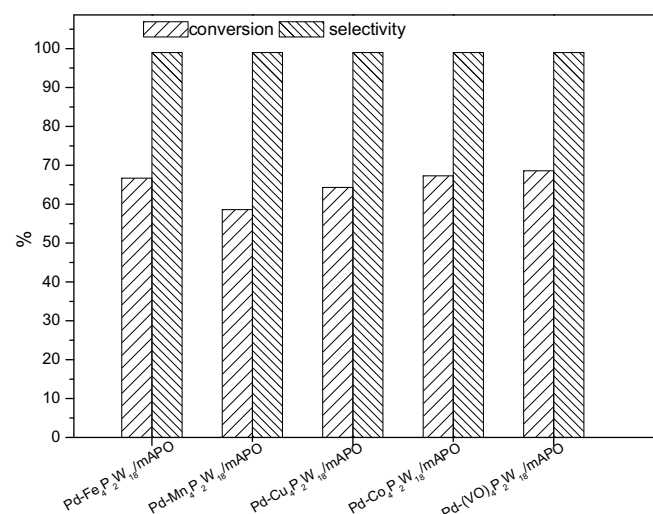


Fig. 8. Catalytic activities of Pd-M₄P₂W₁₈/mAPO with different substituent metal ion in M₄P₂W₁₈ for aerobic oxidation of benzyl alcohol.

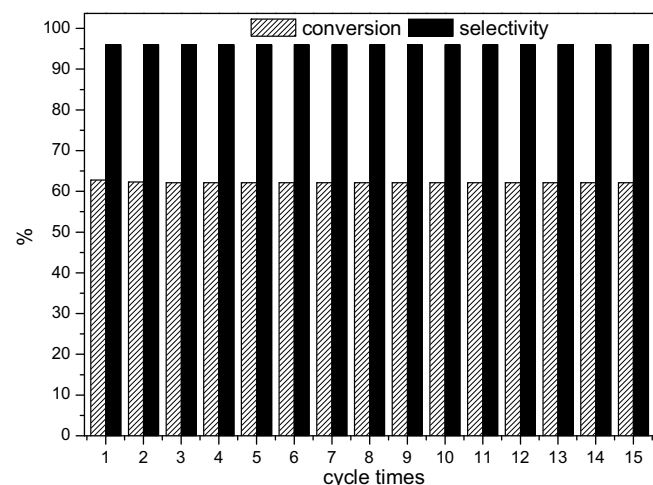


Fig. 9. The recyclability test of Pd-(VO)₄P₂W₁₈/mAPO for aerobic oxidation of benzyl alcohol.

ion substituted M₄P₂W₁₈. The catalytic activity increased with the order: Pd-(VO)₄P₂W₁₈/mAPO > Pd-Co₄P₂W₁₈/mAPO ≈ Pd-Fe₄P₂W₁₈/mAPO > Pd-Cu₄P₂W₁₈/mAPO > Pd-Mn₄P₂W₁₈/mAPO.

Further experiments were performed to test the recyclability of the present catalyst. The consecutive oxidations of benzyl alcohol over the representative Pd-(VO)₄P₂W₁₈/mAPO catalyst were carried out under the same conditions as before. After the first reaction, the catalyst was filtered and the catalyst-free solution was kept under the same reaction conditions for further 12 h. No further increase in conversion was detected and atomic absorption analysis of the remaining solution indicated no Pd and (VO)₄P₂W₁₈ species had leached into the reaction, this clearly suggest the actual catalytic activity of the recovered catalyst is come from the immobilized active centers. The recovered catalyst was used in 15 successive reactions. For each recycle run, the catalyst was recovered by a centrifugation, washed by acetone and dried for the next cycles. The results of conversion and selectivity after each recycling were reflected in Fig. 9. It is found that the catalyst shows excellent recyclability and exhibits the same activity in 15 subsequent reactions. The amount of Pd and polyoxometalates in the recovered Pd-(VO)₄P₂W₁₈/mAPO were further determined to be 0.97 wt% of mAPO and 16.7 μmol/g of mAPO using ICP-AES, respectively, almost remain unchanged compared with fresh Pd-

Table 3Aerobic oxidation of various alcohols using Pd-(VO)₄P₂W₁₈/mAPO.^a

| Entry | substrates | product | mol%Pd | T(°C) | Time(h) | Conv. (%) ^b | Select. (%) ^b |
|-----------------|------------|---------|--------|-------|---------|------------------------|--------------------------|
| 1 | | | 0.5 | 80 | 6 | 55.6 | 98 |
| 2 | | | 0.5 | 80 | 8 | 53.3 | 98 |
| 3 | | | 0.5 | 80 | 12 | 51.5 | 98 |
| 4 | | | 0.5 | 90 | 12 | 47.3 | 97 |
| 5 | | | 0.5 | 90 | 12 | 53.0 | 99 |
| 6 | | | 0.5 | 80 | 12 | 49.8 | 98 |
| 7 | | | 0.5 | 80 | 12 | 43.4 | 98 |
| 8 | | | 0.8 | 100 | 20 | 10.6 | 99 |
| 9 ^c | | | 0.8 | 100 | 20 | 34.5 | 99 |
| 10 | | | 0.8 | 100 | 20 | 9.3 | 99 |
| 11 ^c | | | 0.8 | 100 | 20 | 31.0 | 99 |
| 12 | | | 0.8 | 90 | 20 | 13.3 | 99 |
| 13 ^c | | | 0.8 | 90 | 20 | 38.0 | 99 |

^a Reaction conditions: 1 mmol of alcohol in 10 mL of water, 1 atm of O₂.^b Based on GC.^c Polyethylene glycol/water (4 mL/6 mL) mixture as solvent.

(VO)₄P₂W₁₈/mAPO (the contents of Pd and polyoxometalates in fresh catalyst is 0.97 wt% and 16.8 μmol/g of mAPO, respectively).

The excellent recyclability of Pd-M₄P₂W₁₈/mAPO may be associated with the size and morphology controlling of Pd nanoparticles. TEM images of fresh Pd-(VO)₄P₂W₁₈/mAPO and Pd-(VO)₄P₂W₁₈/mAPO used for four times have not obvious difference in Pd particle size and Pd dispersion, this indicates the stabilization of polyoxometalates and support protection successfully prevent Pd nanoparticles from aggregating into larger particles of Pd black, thus the catalyst can remain its catalytic activity even after twelve times of cycle.

3.2.2. Aerobic oxidation of other alcohols in water

The present Pd-M₄P₂W₁₈/mAPO was also active for the aerobic oxidation of a wide range of alcohols, the representative results using Pd-(VO)₄P₂W₁₈/mAPO as catalyst were summarized in Table 3. Under the investigated conditions, the secondary aromatic alcohol, 1-phenylethanol, 1-phenyl-1-propanol and 1-(4-methoxyphenyl)-1-propanol were oxidized selectively into the corresponding ketone in high conversion (Table 3, entries 1 and 2). The substituted benzyllic alcohol, 2-methoxybenzyl alcohol and 4-methoxybenzyl alcohol also exhibit good catalytic productivity, reached conversion of 47.3% and 53%, respectively (Table 3, entries 3–4). Pd-(VO)₄P₂W₁₈/mAPO also showed good activity for allyl

alcohols. The allyl alcohol substrates such as 3-phenyl-2-propene-1-ol and 3-methyl-2-butene-1-ol afforded the conversions of 68.2% and 66.9%, respectively (Table 3, entries 5 and 6). The high reactivity of allyl alcohol can be ascribed to its structural factor. The allyl alcohols have C=C double bond in their structure, the coordination of C=C double bond to the Pd species can enhance the interaction of hydroxyl group with Pd species [9]. Comparatively, secondary aliphatic alcohols are less reactive than the benzoic ones, 2-hexanol, 2-octanol and cyclohexanol were converted to the corresponding ketones in conversions of 10.6%, 9.3% and 13.3% at higher temperature within 20 h, respectively (entries 4–6, Table 2). But the conversions of these secondary aliphatic alcohols can be enhanced to 34.5%, 31% and 38%, respectively by using polyethylene glycol/water mixed solvent (entries 7–9, Table 3). The improvement of conversion may be ascribed to the increase in solubility of the substrates by adding polyethylene glycol as co-solvent.

4. Conclusion

In this present work, we described a hydrothermal synthesis of a new recyclable and efficient palladium-based catalyst for the aerobic oxidation of alcohols in water by in situ encapsulation of polyoxometalates stabilized palladium nanoparticles in mesoporous aluminophosphate. We also demonstrated the

dual function of polyoxometalates $M_4P_2W_{18}$ in the obtained Pd- $M_4P_2W_{18}$ /mAPO as both stabilizing agent and promoter for palladium nanoparticles. Comparison of activity of Pd- $M_4P_2W_{18}$ /mAPO and Pd + $M_4P_2W_{18}$ /mAPO revealed the stronger interaction of polyoxometalates and palladium nanoparticles resulted in a more efficient synergic effect that led to enhanced activity. It is found the combinations of polyoxometalates and mesoporous channels of support effectively suppressed the agglomeration of palladium nanoparticles and produced a durable catalyst. This approach may find potential applications in other reactions that involving other noble metal nanocatalyst. Efforts for further applications of other nanocatalyst by this approach are now in progress.

Acknowledgement

This research was supported by grants from the natural Science Foundation of China (no. 2140605 and no. 51306047), Hunan Provincial Science and Technology department of China (no. 2014NK3060), Hunan Natural Science Foundation (no. 13JJB009) and state key lab for powder metallurgy.

References

- [1] M. Hudlický, Oxidation in Organic Chemistry, ACS, Washington DC, 1990.
- [2] C. Parmeqiani, F. Cardona, *Green Chem.* 14 (2012) 547–564.
- [3] M.J. Schultz, M.S. Sigman, *Tetrahedron* 62 (2006) 8227–8241.
- [4] I.W.C.E. Arends, G.J. Brink, R.A. Sheldon, *J. Mol. Catal. A: Chem.* 251 (2006) 246–254.
- [5] Z.C. Ma, H.Q. Yang, Y. Qin, Y.J. Hao, G. Li, *J. Mol. Catal. A: Chem.* 331 (2010) 78–85.
- [6] T. Harada, S. Ikeda, F. Hashimoto, T. Sakata, K. Ikeue, T. Torimoto, M. Matsumura, *Langmuir* 26 (2010) 17720–17725.
- [7] Y. Uozumi, R. Nakao, *Angew. Chem. Int. Ed.* 42 (2003) 194–197.
- [8] A. Biffis, L. Minati, *J. Catal.* 236 (2005) 405–409.
- [9] B. Feng, Z.S. Hou, H.M. Yang, X.R. Wang, Y. Hu, H. Li, Y.X. Qiao, X.G. Zhao, Q.F. Huang, *Langmuir* 26 (2010) 2505–2513.
- [10] N. Jamwal, M. Gupta, S. Paul, *Green Chem.* 10 (2008) 999–1003.
- [11] M. Mifsud, K.V. Parkhomenko, I.W.C.E. Arends, R.A. Sheldon, *Tetrahedron* 66 (2010) 1040–1044.
- [12] F. Li, Q.H.Y. Wang, *Appl. Catal. A: Gen.* 334 (2008) 217–226.
- [13] J. Chen, Q.H. Zhang, Y. Wang, H.L. Wan, *Adv. Synth. Catal.* 350 (2008) 453–464.
- [14] D.R. Rolison, *Science* 299 (2003) 1698–1701.
- [15] C. Mondeli, D. Ferri, J.D. Grunwaldt, F. Krumeich, S. Mangold, R. Psaro, A. Baiker, *J. Catal.* 252 (2007) 77–87.
- [16] F. Alardin, B. Delmon, P. Ruiz, M. Devillers, *Catal. Today* 61 (2000) 255–262.
- [17] A.B. Powell, S.S. Stahl, *Org. Lett.* 15 (2013) 5072–5075.
- [18] D. Wang, A. Villa, P. Spontoni, D.S. Su, L. Prati, *Chem. Eur. J.* 16 (2010) 10007–10013.
- [19] S. Marx, A. Baiker, *J. Phys. Chem. C* 113 (2009) 6191–6201.
- [20] Y.T. Chen, Z. Guo, T. Chen, Y. Yang, *J. Catal.* 275 (2010) 11–24.
- [21] T. Harada, S. Ikeda, F. Hashimoto, T. Sakata, K. Ikeue, T. Torimoto, M. Matsumura, *Langmuir* 26 (2010) 17720–17725.
- [22] B. Karimi, S. Abedi, J.H. Clark, V. Budarin, *Angew. Chem. Int. Ed.* 45 (2006) 4776–4779.
- [23] F.F. Bamoharram, A. Ahmadpour, M.M. Heravi, A. Ayati, H. Rashidi, B. Tanhaei, *Synth. React. Inorg. Met. Org. Nano Met. Chem.* 42 (2012) 209–230.
- [24] L. D'souza, M. Noeske, R.M. Richards, U. Kortz, *Appl. Catal. A: Gen.* 453 (2013) 262–271.
- [25] J. Ettedgui, R. Neumann, *J. Am. Chem. Soc.* 131 (2009) 4–5.
- [26] V. Kogan, Z. Aizenshtat, R. Popovitz-Biro, R. Neumann, *Org. Lett.* 4 (2002) 3529–3532.
- [27] A. Corma, S. Iborra, F.X. Llabrés i Xamena, R. Montón, J.J. Calvino, C. Prestipino, *J. Phys. Chem. C* 114 (2010) 8828–8836.
- [28] P.P. Zhao, Y. Leng, M.Q. Zhang, J. Wang, Y.J. Wu, J. Huang, *Chem. Commun.* 48 (2012) 5721–5723.
- [29] D. Barats, R. Neumann, *Adv. Synth. Catal.* 352 (2010) 293–298.
- [30] M. De bruyn, R. Neumann, *Adv. Synth. Catal.* 349 (2007) 1624–1628.
- [31] R. Liu, S. Li, X. Yu, G. Zhang, S. Zhang, J. Yao, L. Zhi, *J. Mater. Chem.* 22 (2012) 3319–3322.
- [32] R. Neumann, *Inorg. Chem.* 49 (2010) 3594–3601.
- [33] R.G. Finke, M.W. Droege, P.J. Domaille, *Inorg. Chem.* 26 (1987) 3886–3896.
- [34] C. Ornelas, J. Ruiz, L. Salmon, D. Astruca, *Adv. Synth. Catal.* 350 (2008) 837–845.
- [35] M.S. Balula, J.A. Gamelas, H.M. Carapuça, A.M.V. Cavaleiro, W. Schlindwein, *Eur. J. Inorg. Chem.* 3 (2004) 619–628.
- [36] J.M. Campelo, M. Jaraba, D. Luna, R. Luque, J.M. Marinas, A.A. Romero, *Chem. Mater.* 15 (2003) 3352–3364.
- [37] I.C.M.S. Santos, J.A.F. Gamelas, M.S.S. Balula, M.M.Q. Simões, M.G.P.M.S. Neves, J.A.S. Caveleiro, A.M.V. Cavaleiro, *J. Mol. Catal. A: Chem.* 262 (2007) 41–47.
- [38] N.M. Okun, T.M. Anderson, C.L. Hill, *J. Am. Chem. Soc.* 125 (2003) 3194–3195.